

Pulsed Nd:YAG laser selective ablation of surface enamel caries: I. Photoacoustic response and FTIR spectroscopy

David M. Harris, Daniel Fried

Department of Restorative Dentistry, University of California San Francisco, San Francisco, CA 94143

ABSTRACT

Enamel caries lesions on extracted teeth were ablated with a pulsed Nd:YAG or Er:YAG laser. Tissue ablation was accompanied by a “popping” sound (the photoacoustic response). Analysis of the photoacoustic response yields insights into the laser / tissue interactions. Fourier Transform Infrared (FTIR) Spectroscopy of lesions before ablation show a strong protein component associated with organic material (i.e., bacteria). Following ablation this protein component is absent.

KEYWORDS: Enamel caries, laser selective ablation, photoacoustic, selective photothermolysis.

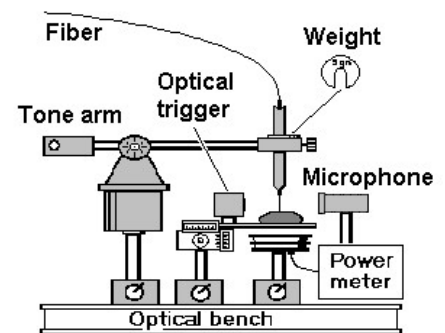
1. INTRODUCTION

Enamel caries appears darker than the surrounding normal tissue mainly due to the presence of pigmented anaerobic bacteria and their metabolic byproducts, the primary pigment being melanin. In skin melanocytes have been shown to absorb 1.064 μm laser energy (pulsed Nd:YAG), and can be selectively ablated by the process of selective photothermolysis.¹ Selective ablation of dentinal caries has been demonstrated quantitatively in the UV-VIS range¹⁻⁵ and selective ablation of enamel caries in the near IR (pulsed Nd:YAG) has been described clinically.⁶⁻¹⁰

The current standard of practice for treatment of enamel caries is removal with the dental highspeed hand piece (dental drill). The endpoint of this procedure is the removal of all pigmented enamel, determined visually. It has been shown that this method successfully removes caries but also removes healthy, albeit stained, enamel below the lesion.¹⁰ Removal of enamel caries by pulsed lasers offers the potential of a more conservative procedure than the drill by selectively sparing normal tissue.

Laser light absorption and ablation characteristics were observed for carbon, dentin, enamel and enamel caries. The photoacoustic response was measured to determine the relative absorption and ablation characteristics at $\lambda=1.064 \mu\text{m}$ (Nd:YAG) and 2.94 μm (Er:YAG). Subjectively, the photoacoustic response is the audible “pop” (increase in sound intensity) heard when a pulsed laser impacts dental hard tissue. Objectively, the measured magnitude (dB SL) of the response is correlated with the amount of tissue ablated.^{1,11} Prior to ablation FTIR spectroscopy was used to identify the absorption spectrum of surface enamel caries. Post-laser spectroscopy was used to verify caries removal.

Figure 1. Experimental setup for irradiation and recording the photoacoustic response. The fiber from the Nd:YAG laser was held in contact with the sample with a constant force. The non-contact Er:YAG fiber was positioned to provide an 800 mm spot size.



2. METHODS

The samples irradiated were graphite (carbon), normal dentin, healthy enamel and pigmented pit and fissure enamel caries selected by a dentist from extracted human molars.

The output from a PulseMaster free-running pulsed Nd:YAG laser (American Dental Technologies, Inc. Southfield, MI) with pulse energies up to 0.32 Joules was delivered through a 300 μm diameter silica fiber in contact with the tissue. The fiber delivery handpiece was attached to a phonograph tone arm to provide a uniform force of 20 grams at the fiber/tissue

interface. Previous work has established that ablation rate on dentin is insensitive to pressure over the range 15-50 gms.^{12,13} Spot size equaled fiber diameter.

A Continuum Er:YAG laser (Santa Clara, CA) had pulse energies of up to 500 mJ. Irradiation was delivered free-beam with a 600 μm diameter fluoride fiber with a low OH tip placed close to the sample. Spot size was approximately 800 μm . There were no focusing optics with either laser system.

The energy output of both lasers was monitored with a calibrated, Molecron ED-200 pyroelectric calorimeter. A Molecron P5 ultrafast pyroelectric with a rise time of 500 ps was used to resolve the micropulses.

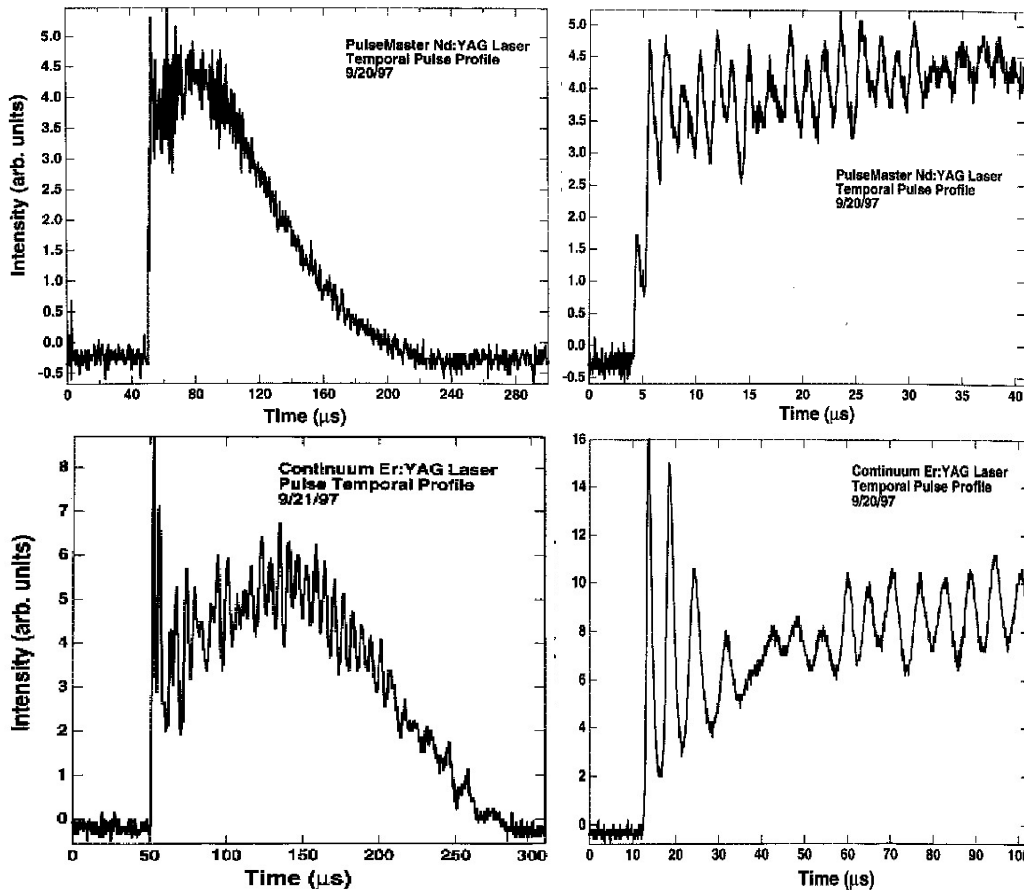


Figure 2. Temporal pulse structure of free-running pulsed Nd:YAG (top) and Er:YAG. (bottom). Note the different time scales illustrating the duration of micropulses (right).

A microphone (Model #4012, ACO Pacific, Belmont, CA) was used free-field to record the sound generated during laser irradiation of the samples. The time-resolved waveform was acquired using a digital oscilloscope interfaced to a computer and the digitized waveforms were used for comparison of the various laser irradiation parameters. A boxcar integrator module was used to sample and hold the peak voltage of the selected component of the acoustic signal. The temporal window (gate) at which the microphone signal was acquired and held by the integrator module is shown in Fig. 2 superimposed with the waveform of the microphone response. Plots are provided of the acoustic waveform. The “acoustic response” is represented as a graph of the integrated amplitude of the first component over time. All pulses were delivered at a repetition rate of 10 Hz. The fiber was maintained in a fixed position and samples were irradiated for 20 seconds (200 pulses).

Fourier Transform infrared (FTIR) spectroscopy was performed with a Laser Precision RXF-30 FTIR Microscope in the reflective mode. Specular reflectance FTIR spectroscopy requires a parallel-plano tissue surface so that light reflected from the sample surface can be directed to the detector. Due to this constraint, FTIR spectroscopy was performed on faceted

samples of interproximal enamel caries that provided a flat surface parallel to the detector. Spectroscopy was performed before and after irradiation with the pulsed Nd:YAG.

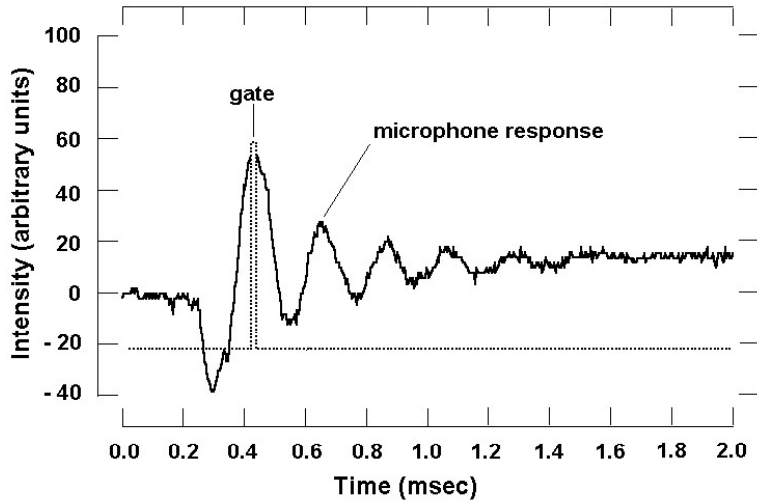


Figure 3. Signal processing of microphone signal using a Boxcar Integrator/Averager. The peak voltage is sampled during the first positive pressure transient using a sample and hold circuit at the designated gate position. The voltage is subsequently amplified and transferred to either a digital oscilloscope or a computer to record the magnitude of the acoustic response for a specific laser pulse. Histograms were compiled from these values that illustrate the magnitude of the photoacoustic response to sequential pulses.

4. RESULTS

4.1 Temporal pulse profile.

Console settings are reported here and can be corrected with a simple multiplicative scaling factor (.75) since the output of both lasers increased linearly with the respective energy settings. The temporal pulse structures are shown in Figure 2. For the Nd:YAG laser the pulse duration was approximately 150 μ s (FWHM) and the Er:YAG was 200 μ s. The micropulse durations (peak-to-peak) were about 1.4 μ s for the Nd:YAG and about 5.7 μ s for the Er:YAG.

4.2 Acoustic responses to Nd:YAG Irradiation.

The acoustic waveforms generated on graphite, dentin and healthy enamel are shown in Figure 4. The latencies of the first positive peak (rarefaction) varied little from one material to the next but amplitudes were quite different. The magnitude was greatest on graphite due to the strong absorption at 1064 nm., lower on dentin, and several orders of magnitude weaker on healthy enamel.

Sequential pulses on graphite initially evoked loud acoustic transients that diminished to baseline within 3-4 seconds (not shown). Plots of the amplitude of the response for sequential pulses are shown for dentin and enamel in Figures 5. In the case of dentin the signal was initially weak and gradually gained strength. Then the signal magnitude gradually decreased in a similar matter to that observed for graphite. Acoustic responses to irradiation of sound enamel were very weak. Note that the enamel trace is magnified 10X in the figures for comparison. Occasionally, there would be a signal on normal enamel, probably as the laser impacted a slightly stained area or a dust particle.

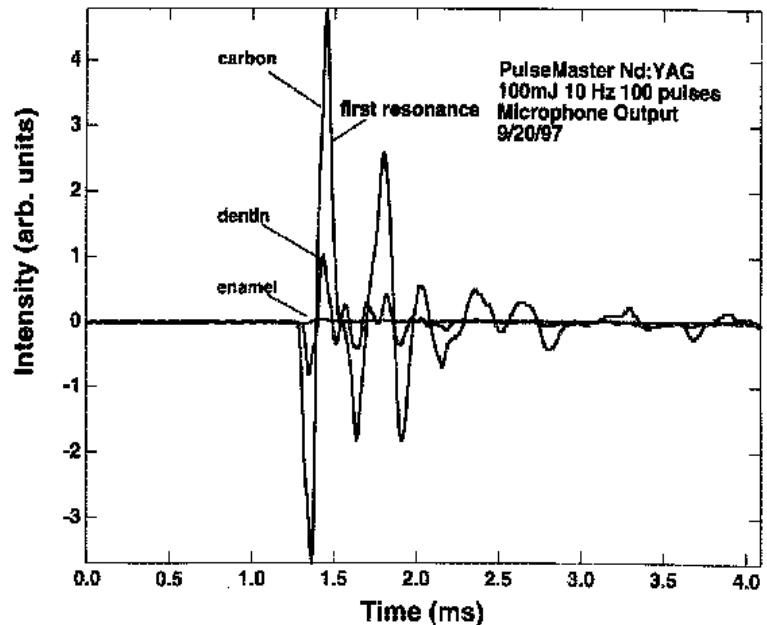


Figure 4. Averaged acoustic response to 100 pulses of the Nd:YAG laser at 100 mJ. The amplitude is related to the absorption (and ablation) characteristics.

A modified protocol was used to collect the data for enamel caries shown in figure 6. Instead of maintaining the fiber at a single location it was moved across the lesion as would be done in a clinical application. There were strong signals as the laser energy was absorbed and vanished after these "ablative" laser pulses removed the pigmented tissue.

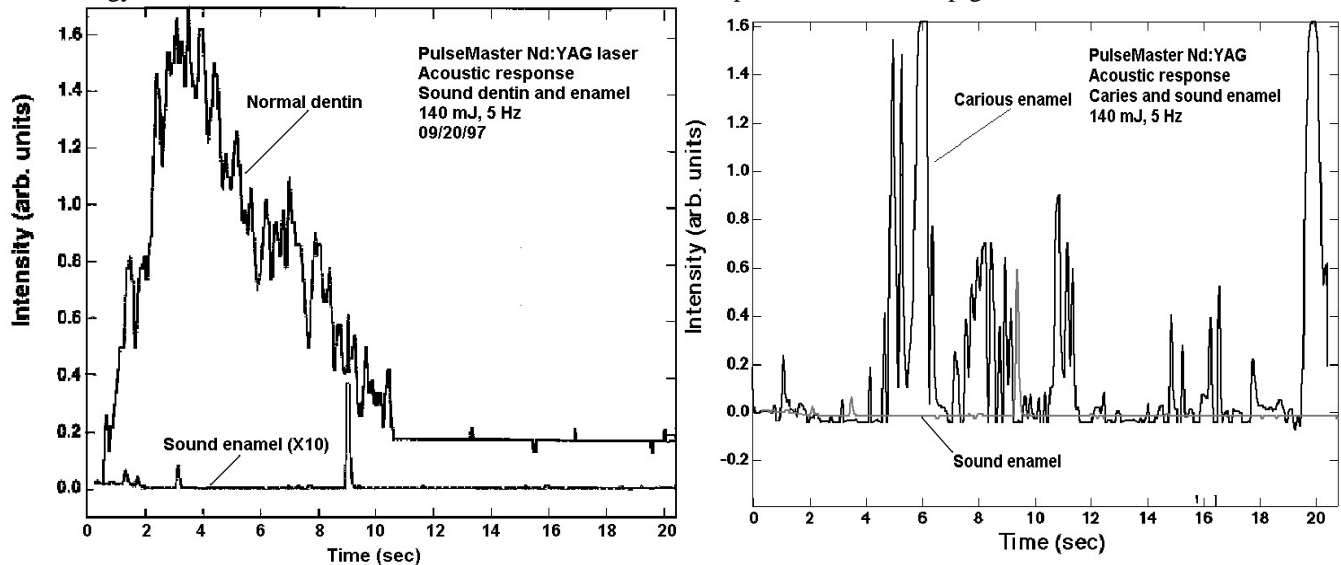


Figure 5. Histograms of the magnitude of the photoacoustic response to sequential Nd:YAG laser pulses at 140 mJ, 5 Hz. Right: Acoustic responses to irradiation of normal dentin compared to normal enamel (X10). Left: Cariou enamel compared to sound enamel.

4.3 Acoustic responses to Er:YAG Irradiation.

The response on graphite was much weaker at 2.94 μm than that at 1.064 μm . We suspect that this is due to the larger spot size coupled with the fact that the fiber was not placed in contact with the graphite. The signal subsequently decayed in a similar manner to that observed during 1.064 μm laser irradiation, presumably due to morphological changes induced in the graphite.

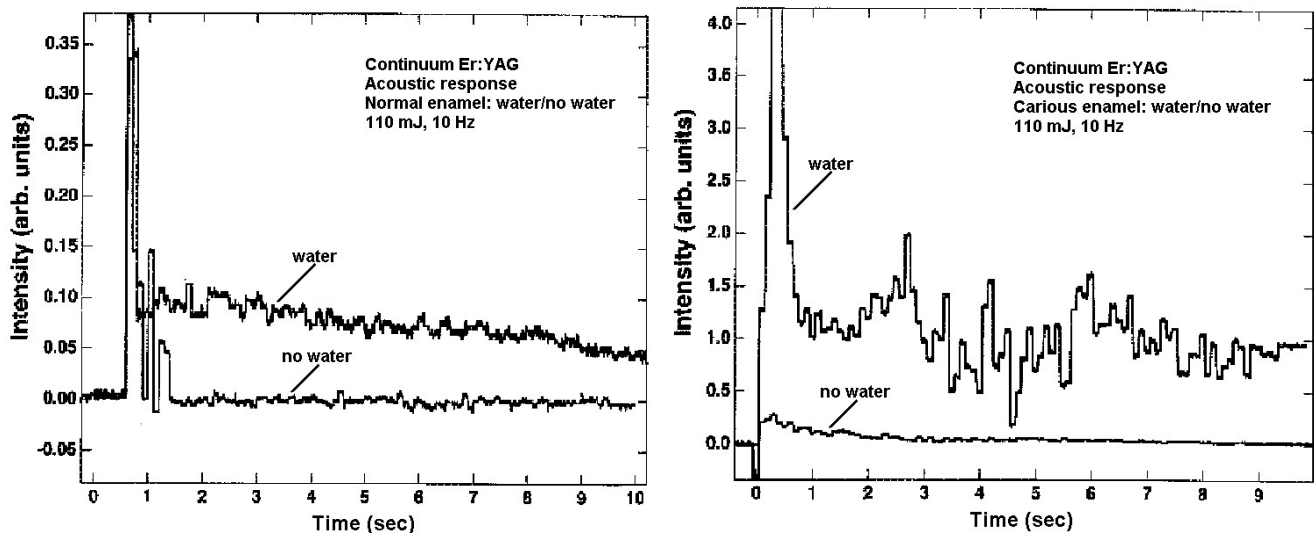


Figure 6. Histograms of the magnitude of the photoacoustic response to sequential Er:YAG laser pulses at 110 mJ, 10 Hz. Right: Acoustic responses to irradiation of normal enamel with and without water. Left: Cariou enamel with and without water.

The magnitude of the acoustic response on dentin was very strong and, in contrast to Nd:YAG, there was no incubation period observed. The first few pulses were the strongest followed by a gradual drop in the magnitude of the acoustic signal (Figure 6). This may indicate that the laser energy is coupling into the water in the tissue itself and that changes in tissue morphology may not affect ablation.

A. Caries: pre-ablation

B. Debris: post-ablation

C. Debride and acid etch

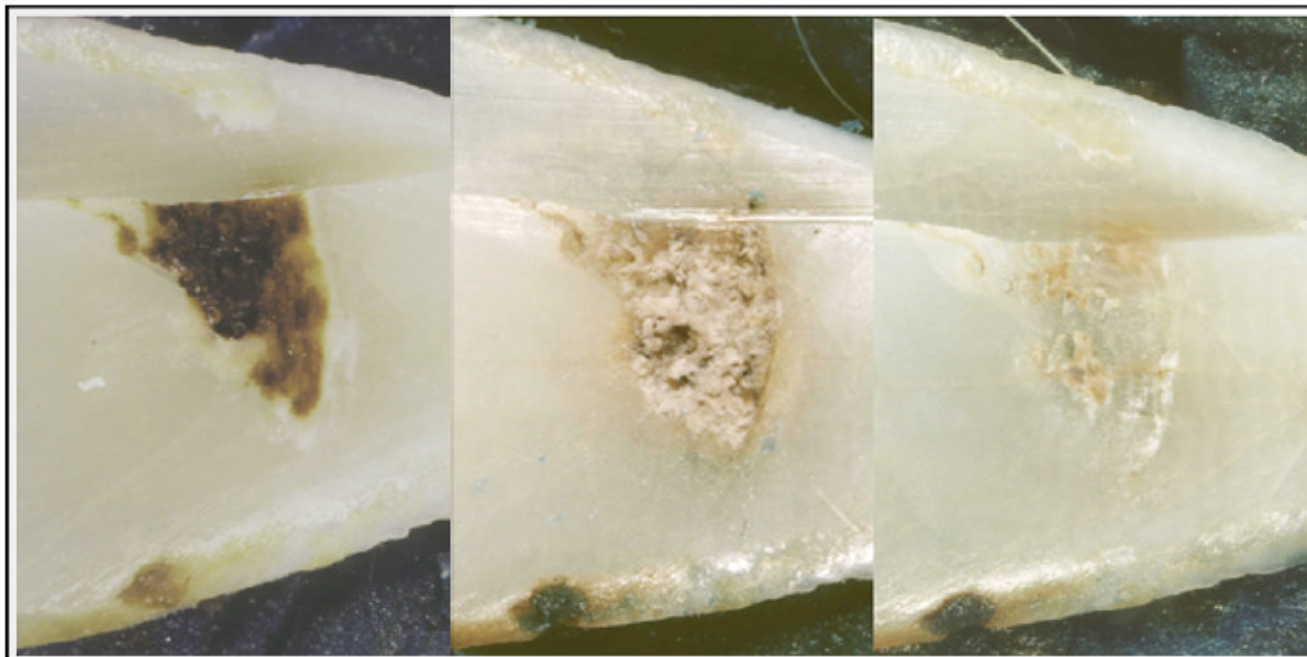


Figure 7A. Dental caries. B. Pulsed Nd:YAG ablation by-products (160 mJ, 10 Hz). C. Debris removed with acid etch and polishing. Enamel surface was faceted for reflection spectroscopy.

Plots of the acoustic responses observed for Er:YAG impact on normal and carious enamel were very similar with a few strong initial pulses followed by a gradual decrease in the signal magnitude. For all samples irradiated with Er:YAG the signal magnitude increased at least an order of magnitude when water was present in the sample surface due to the strong coupling of the water at 2.94 μm . It is interesting to note that it typically requires several laser pulses to remove the water.

4.4 FTIR Spectroscopy

Figure 7 is a macroscopic photograph showing a sample of an interproximal caries lesion used for the spectroscopy study. Figure 7A is the lesion before removal with the PulseMaster. Figure 7B shows the surface debris immediately after irradiation. Figure 7C shows a sound enamel surface that remains after acid etching has removed the surface debris. Note that discolored sound enamel is revealed after removal of the lesion.

Five samples with superficial enamel caries were evaluated spectroscopically before and after irradiation with the pulsed Nd:YAG laser at 100mJ, 10Hz. Figure 8 shows representative spectra. The presence of water is indicated by signal below 6 μm , protein (amide bands, carbonate) in the 6-8 μm band, and phosphate in the 9-10 μm band. A spectrum of normal adjacent enamel shows a lack of absorption in the range 6-9 μm . The absorption of carious enamel shows a strong protein component presumably associated with the presence of bacteria and organic debris. Following irradiation the protein component at the lesion site is removed and spectra resemble that of sound enamel.

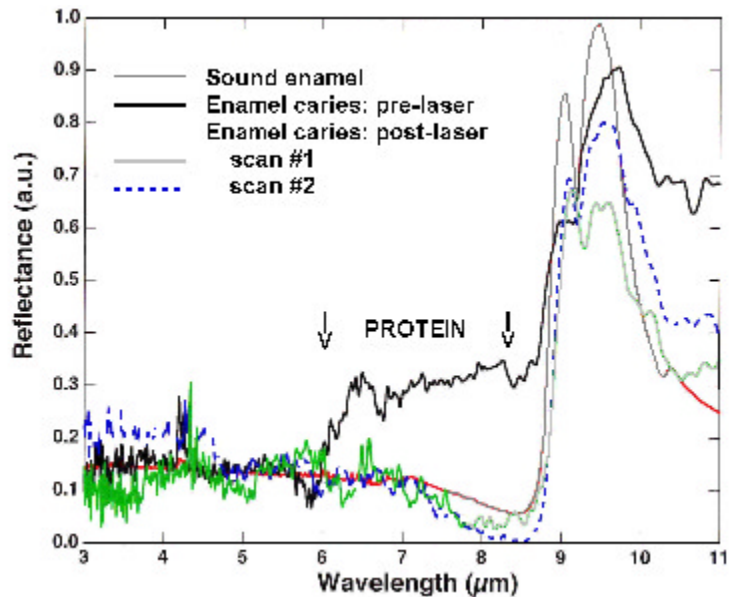


Figure 8. Fourier Transform Infrared Spectroscopy of enamel caries showing protein component prior to ablation that disappears after Nd:YAG irradiation. Spectrum of normal enamel shown for comparison.

5. DISCUSSION

Photoacoustic methods measure the acoustic wave that is generated when a laser pulse is absorbed by the target tissue. The signal generated is proportional to the incident intensity, absorption co-efficient, thermal diffusivity and modulation frequency. The absorption of laser energy induces a change of state of the target from the solid or liquid state to the gas or vapor state. The acoustic signal is generated by thermal elastic expansion or, above ablation threshold, by the explosive expansion of water and/or vaporized organic material.¹

The optical properties of dental hard tissues in the visible and near infrared are dominated by light scattering, that is, scattering coefficients exceed absorption coefficients by orders of magnitude. Estimates of absorption coefficients require extensive numerical modeling to extract probable absorption coefficients from angularly resolved transmission and scattering measurements. As a result, direct optical transmission and reflective methods are extremely difficult to implement on dental hard tissues. Measurement of the photoacoustic response (acoustic response to pulsed laser impact) provides a simple tool for measuring the relative absorption of carious and noncarious dental hard tissue.³⁻⁶ Additionally, it is a sensitive method for detecting the respective ablation thresholds for various tissues.¹⁴⁻¹⁷ Above ablation threshold the signal increases by orders of magnitude due to the explosive release of gases and plume ejecta.

These studies indicate that the acoustic signature produced during the laser irradiation of dental hard tissue can also be used to provide information about laser-tissue interactions. A strong characteristic acoustic signature is produced upon ablation of tissue and reflects the absorption characteristics of the target determined by tissue chromophores, or any absorber applied

to the surface. The magnitude of the acoustic signal reflects the energy absorbed by the target and the subsequent pressure rise at the tissue surface. The acoustic signal also reflects the energy released during the explosive expansion of the target tissue with small ejected particles.

Monitoring the magnitude of the photoacoustic signal as a function of the number of laser pulses provides important information about the evolving absorption characteristics of the tissue. During ablation of graphite the signal is initially high due to the strong absorption. Photoacoustic magnitude falls off gradually as a crater is formed and the surface topography changes markedly. For dentin there is initially a weak signal due to the poor absorption, followed by an increase in absorption as the protein chars creating a highly absorbing target. After reaching maximum intensity, the signal drops as the char is ablated and an ablation crater is created. Thermal modification of the tissue changes its absorption characteristics and crater formation increases the irradiated surface area (decreases incident fluence). Therefore, the photoacoustic response is an excellent tool for determining both the onset of ablation and subsequent "stallout" after thermal modification of the tissue.

For the ablation of normal enamel there is a very small signal since enamel absorbs poorly at 1.064 μm and the incident fluence needed for ablation is not achieved. If the tissue is pigmented as with caries, then there is a strong acoustic signal for the first one or two laser pulses as the pigmented tissue is ablated away; followed by no signal indicative of cessation of ablation.

The mechanisms of acoustic wave generation during Nd:YAG or Er:YAG laser ablation are probably quite different. The Nd:YAG laser vaporizes the pigmented organic/mineral matrix in the fissure leading to ablation and the rapid expansion of spallated and vaporized material. In the case of the Er:YAG laser, the laser energy couples to the water in the tissue heating it beyond the vapor point. This creates subsurface pressures that exceed the tensile strength of the enamel causing it to fly apart with high energy. For both lasers the ablated material creates strong pressure waves as it rapidly pushes against the background gas. In the case of Er:YAG ablation of a carious lesion, since water is the primary chromophore at 2.94 μm , pigmentation does not influence the absorption significantly. Therefore, the Er:YAG laser is selective to the presence or absence of water but not to the presence or absence of enamel caries.

Photoacoustic measurements and spectroscopy both support the assumption that the Nd:YAG laser is absorbed by and ablates pigmented tissue. With enamel caries ablation will cease once the pigment is removed and the laser pulses encounter normal enamel. Therefore, pulsed Nd:YAG laser ablation of enamel caries is both selective and self-limiting. The clinical endpoint is auditory, the practitioner knows the target is ablated when he can no longer elicit a photoacoustic response.

ACKNOWLEDGMENT

This research was supported by a grant from American Dental Technologies, Inc., Southfield MI 48034 and NIDCR R29-DE12091.

REFERENCES

1. RR Anderson, RJ Margolis, S Watanabe, T Flott, GJ Hruza, JS Dover. Selective photothermolysis of cutaneous pigmentation by Q-switched Nd:YAG laser pulses at 1064, 532, and 355 nm. *J Invest Dermatol* 93(1):28-32, 1989.
2. MK Arima, K Matsumoto Effects of ARF:Excimer laser irradiation on human enamel and dentin. *Laser Surg Med* 13:97- 105, 1993.
3. T Hennig, P Rechmann, C Pilgrim, H-J Schwartzmaier, R Kaufmann. Caries selective ablation by pulsed lasers. *Proceedings SPIE* 1424:99-105, 1991.
4. T Hennig, P Rechmann, CH Pilgrim, and R Kaufmann, Basic principles of caries selective ablation by pulsed lasers, *Proceedings of the Third International Congress on Lasers in Dentistry*, pp. 119-120, Salt Lake City, 1992.

5. T Hennig, P Rechmann, P Jeitner, and R Kaufmann, Caries selective ablation: the second threshold, *Lasers in orthopedic, dental, and veterinary medicine II*, Proc. SPIE, Vol. 1880:117-124, 1993.
6. P Rechmann, TH Hennig, U von den Hoff, and R Kaufmann, Caries selective ablation: 377 nm vs. 2.9 μm , *Lasers in Orthopedic and Veterinary Medicine II*, Proc SPIE, Vol. 1880:235-239, 1994.
7. TD Myers and WD Myers. In Vivo caries removal utilizing the YAG laser. *J Mich Dent Assoc* 67:66-69, 1985a.
8. TD Myers and WD Myers . The use of a laser for debridement of incipient caries. *J Prost Dent* 53:776-779, 1985b.
9. K Matsumoto, T Nakayama. A morphological study on the enamel and dentin irradiated by pulsed Nd:YAG laser (D-Lase 300). ISLD Proceedings Third Int'l Congress on Lasers in Dentistry, Salt Lake City, UT 135-136, 1992
10. KHP Lee, WS Chao, KT Tran, TD Myers, JM White. Caries removal and restoration using Nd:YAG laser and air abrasion. *J Dent Res* 75:91, 1996.
11. R Hibst and U Keller. Experimental studies of the application of the Er:YAG laser on dental hard substances: Measurement of the ablation rate. *Laser Surg Med* 9:335-344, 1989.
12. DM Harris. Contact pulsed Nd:YAG laser ablation of human dentin: ablation rates and tissue effects. Proc SPIE 2128:409-415, 1994.
13. DM Harris. Contact pulsed Nd:YAG laser ablation of human dentin: fiber tip and crater morphology (SEM). Proc SPIE 2128:416-423, 1994
14. PE Dyer and RK Al-Dhahir, Transient photoacoustic studies of laser tissue ablation, *Laser-Tissue Interaction*, Proc SPIE 1202:46-60, 1990
15. CKN Patel and AC Tam. Applications of photoacoustic sensing techniques, *Rev. Modern Phys.*, Vol. 58(2):381-431, 1986.
16. CE Yeack, RL Melcher, and HE Klauser, Transient photoacoustic monitoring of pulsed laser drilling, *Appl. Phys. Lett.* 41:1043-1044, 1982.
17. Petzoldt, AP Elg, M Reichling, J Reif, and E Matthias, Surface laser damage thresholds determined by photoacoustic deflection, *Appl. Phys. Lett.* 53(21):2005-2007, 1988.

CORRESPONDENCE: David M. Harris, bmcinc@earthlink.net; <http://www.biomedicalconsultants.com>.